Structural Engineering and Mechanics, Vol. 33, No. 4 (2009) 503-527
DOI: http://dx.doi.org/10.12989/sem.2009.33.4.503

Investigation on the flexural behaviour of ferrocement pipes and roof panels subjected to bending moment

Alnuaimi A.S.†, Hago A.W., Al-Jabri K.S. and Al-Saidy A.H.

Civil and Architectural Engineering Department, College of Engineering, Sultan Qaboos University, Sultanate of Oman

(Received July 8, 2008, Accepted September 8, 2009)

Abstract. This paper presents experimental results on the behaviour and ultimate load of fifteen pipes and six roof panels made of ferrocement. Additional results from three roof panels, carried out by others, are also compared with this research results. OPC cement, natural sand and galvanised iron wire mesh were used for the construction of 20 mm thick specimens. The pipe length was 2 m and roof panel length was 2.1 m. The main variables studied were the number of wire mesh layers which were 1, 2, 3, 4 and 6 layers, the inner pipe diameter which were 105, 210 and 315 mm, cross sectional shape of the panel which were channel and box sections and the depth of the edge beam which were 95 mm and 50 mm. All specimens were simply supported and tested for pure bending with test span of 600 mm at mid-span. Tests revealed that increasing the number of wire mesh layers increases the flexural strength and stiffness. Increasing the pipe diameter or depth of edge beam of the panel increases the cracking and ultimate moments. The change in the pipe diameter led to larger effect on ultimate moment than the effect of change in the number of wire mesh layers. The box section showed behaviour and strength similar to that of the channel with same depth and number of wire mesh layers.

Keywords: ferrocement; fibre reinforcement; ferrocement pipes; ferrocement panels; bending.

1. Introduction

Ferrocement is a form of thin reinforced concrete material made from mortar and layers of thinly spaced steel rods or wires. The layers behave together as a composite, in which the concrete's integrity is increased with the presence of wire mesh layers. This increases the tensile strength of the composite. One of the main differences between the ferrocement and reinforced concrete is that the ferrocement can be used to construct thin members (in the range of 10 mm) due to the absence of coarse aggregate and conventional reinforcing bars.

Large number of population in many developing countries live under conditions of shortage of potable water and inadequate sanitation facilities as well as indecent dwellings without appropriate roofing, wall and floor systems. One major reason for this situation is the high cost of imported materials.

In arid areas where fresh water is scarce and is mostly found from springs or aquifers, containing

† Corresponding author, E-mail: alnuaimi@squ.edu.om

the available water and transporting it in a cheap and decent pipeline system is a major problem to farmers in many developing countries. The cost of such system is very high compared with the available amount of water. In addition, the use of local materials has not been very successful in producing durable and resistant to fire, insects, and flood especially for roofing materials.

Many researchers have studied the behaviour and ultimate strength of ferrocement under different environmental and loading conditions. Tests included strength, ductility, and resistance to fire and chemicals and carried out cost comparison between ferrocement and conventional concrete.

Iorns (1989) made quality and cost comparisons between different types of materials used in construction and laminated ferrocement. He concluded that laminated ferrocement is more crack-resistant and durable than normal concrete and much less expensive than any of the other materials used now for seawater pipes, tanks, machinery housing, pressure vessels and vacuum chambers.

The ACI Committee 549-IR97 (1997) produced a state of art report on ferrocement and a guide for design while the ACI Committee 549-IR93 (1993) produced a guide for construction and repair of ferrocement. The International ferrocement Centre (IFC) publishes a quarterly journal "Ferrocement".

Memon *et al.* (2007) explored the possibility of reducing the porosity of ferrocement mortar and therefore increasing the compressive strength, while maintaining good workability by addition of superplasticizier. Results showed that the high workability slag cement mortars of reasonably high strength low water absorption and exhibiting early age strength comparable to that of OPC mortars can be designed in order to cast thin ferrocement elements by the method of pouring.

Shui (1989a) experimentally studied the use of ferrocement pipes for subsurface drainage for agricultural use. He concluded that cracking load of the pipes of various diameters considered is not significantly different for the varying number of layers of wire mesh. As the pipe diameter increases, the strength decreases. An empirical design equation for pipe thickness and diameter was established.

Sander *et al.* (1985) used ferrocement covers to protect the district heating pipes against mechanical damage and ground water. The covering ferrocement pipes were pre-cast and used as casing for the underground pipe network which supplies hot water to the household and places of work in Warsaw, Poland. They concluded that the use of such casings is so beneficial in the cost, handling, weight and water tightness.

Duggal (1998) studied the use of bamboo-based ferrocement pipes in water supply pipe networks. The materials used in construction of these pipes are cement, sand, water, wire mesh and bamboo strips. The bamboo strips were used in the central grid and circular rings (hoop rings). He tested two types of pipes; one with 2 layers of wire mesh and the other with 4 layers of wire mesh. He concluded that bamboo-ferrocement pipes can be used effectively as an alternative to conventional RC in case of water supply pipes. They can withstand higher hydrostatic pressure than RC pipes of class P1 and class P2 and resist bearing load higher than RC pipes. They are also cheaper than RC pipes.

Wei (1985) investigated the use of glass fibre reinforced plastic Ferrocement (GRPF) in irrigation. He concluded that coating the ferrocement members with GRP increased the safety, durability, lightness and resistance to cracks of the members.

Ismail and Waliuddin (1996) studied the behaviour of drainage network with ferrocement as lining system for five years. The network was used for disposal of an aggressive animal refuse/dung for dairy farms in Karachi, Pakistan. They concluded that satisfactory results were achieved and recommended the use of sulphate resisting cement in the ferrocement.

Moita *et al.* (2003) analysed the behaviour of large ferrocement water tanks experimentally and

proposed a numerical model for the analysis. They reported large discrepancies between numerical and experimental results due to imperfection in wall thickness and mechanical properties of material as these depend on the skilfulness of the workers. They concluded that a two-dimensional model for analysis would be sufficient to calculate the stress and strain distribution in these structures.

For roofing, ferrocement has been used in the construction of channel type sections, folded plates, ribbed slabs, cylindrical shells, circular domes, funicular shells etc Al-Sulaimani and Ahmad (1988). The use of hollow box section as a roofing element has been investigated by Mathews *et al.* (1991). A total of 21 ferrocement box sections were tested under symmetrical line loads applied at one third span points. The test results confirm that the ferrocement box hollow sections have adequate strength, stiffness and other serviceability requirements for residual applications. Also the theoretical values of cracking load, ultimate load, deflection and crack width at working load showed good agreement with experimental values. Kenai and Brooks (1994) carried out extensive testing on direct tensile, four point flexural and drop impact tests on specimens reinforced with steel wire meshes (13 and 25 mm thick). They used a simple model based on plastic analysis which was originally proposed by Mansur and Paramasivam (1985). The model employed a rectangular stress block in the compression zone and the neutral axis depth was calculated by considering the equilibrium of tension and compression forces. The ultimate moment was calculated by multiplying any one of the two forces by the lever arm. Such models cannot be used in cases where the reinforcing mesh is dispersed in the middle of the slab, because of the small thickness of the ferrocement slab panels (about 20 mm) which makes it is practically difficult to control the uniform dispersion of the wire mesh through the depth. Hago *et al.* (2005) studied the ultimate load and behaviour of ferrocement roof slab panels. Three flat slabs and three channel slabs with edge beams of 50 mm were tested. The parameters studied included: the effect of the percentage of wire mesh reinforcement by volume and the structural shape of the panels on the ultimate flexural strength, first crack load, crack spacing and load-deformation behaviour. The results demonstrated that the monolithic shallow edge ferrocement beams with the panels considerably improves the service and ultimate behaviour, irrespective of the steel layers used. Also, slabs with channel sections supported larger ultimate loads and behaved better under service loads than their flat slabs counterparts. Due to large deflections experienced by the thin panels, large deflection theory was adopted in the analysis. Good agreement was obtained between the theoretical and experimental ultimate loads using the proposed mathematical model.

Yen and Su (1980) studied the effect of skeletal steel bars and wire mesh layers on the flexural behaviour of ferrocement panels. The panel's width ranged from 149 mm to 184 mm and the thickness was between 22 mm to 62 mm. They concluded that the skeletal steel increases the ultimate strength.

Al-Kubaisy and Jumaat (2000) studied the flexural behaviour of reinforced concrete slabs with ferrocement tension zone cover. Twelve simply supported slabs were tested. The slabs were rectangular with 500 mm width, 75-85 mm total depth and total length of 1500 mm. They concluded that reinforced concrete slabs with ferrocement tension zone cover is superior in crack control, stiffness and cracking moment to similar slabs with normal concrete cover.

Masood *et al.* (2003) studied the performance of ferrocement slab panels in different environments. The panels were cast with varying number of woven and hexagonal mesh layers and tested for flexure. Control specimens were cast and cured with potable water while other specimens were cast and/or cured with saline water to create moderate and hostile environments. In normal casting and curing environment, the addition of fly ash, for more than 20%, as replacement to

cement was found to decrease the strength. However, the addition of fly ash was found to slightly increase the strength in normal casting and saline curing, and in saline casting and curing specimens. The fly ash was found to minimize the ingress of water during casting and therefore produce better pore structure.

Greepala and Nimityongskul (2008) studied the structural integrity of ferrocement panels exposed to fire. Results showed that ferrocement jackets with different number of wire mesh layers possessed better post fire strength compared with plain mortar. Unlike in normal conditions, the number of mesh layers had insignificant effect on the mechanical properties after fire exposure.

Shannag (2008) tested, for flexure, ferrocement plates with varying number of wire mesh layers (2 and 4 layers) and immersed in sodium and magnesium sulphate solutions, and tap water for a period of one year. Results showed that, after one year of storage in sulphate solutions, the specimens reinforced with two layers of wire meshes, showed a significant increase in flexural strength accompanied with a noticeable decrease in ductility for specimens reinforced with medium and large wire spacings, whereas most of the specimens reinforced with four layers showed some decrease in flexural strength and ductility compared to the specimens stored in tap water.

The punching shear strength of ferrocement panels was studied by Mansur *et al.* (2001). They tested 31 square panels using central concentrated load on simply supported panels. Results showed that all slabs failed first in punching without total separation, and then exhibited a second peak in load deflection history. Both cracking load and punching shear load increased with an increase of width of the square load area, mortar strength, volume fraction of reinforcement, and the depth of the slab but decreased as the effective span was increased. The critical perimeter for punching shear failure was found to be located at 1.5 times the thickness of the slab from the edge of the loading plate.

Silva *et al.* (2004) tested the tensile strength of ferrocement panels reinforced with grid wires using Weibull model. It was assumed that the data from 33 tested panels were linear elastic. It was shown that all experimental data could be plotted in a unique modified Weibull diagram in which the relevant stress to consider is the so-called Weibull stress.

Paramasivam *et al.* (1998) tested the use of ferrocement laminates as strengthening components for RC beams. Results showed that the addition of ferrocement laminates to the tension side of the beam substantially increased the cracking moment and resulted in narrower cracks.

Abdullah and Takiguchi (2003) investigated the behaviour and strength of reinforced concrete columns strengthened with ferrocement jackets. They found that no flexural strength enhancement was achieved due to strengthening of R/C columns with ferrocement regardless of the number of wire mesh layers. The shear resistance of R/C columns with inadequate shear reinforcement was improved with presence of ferrocement jacketing. Similar results were found by Kazemi and Morshed (2005) who studied the seismic shear strengthening of R/C columns with ferrocement jacket reinforced with expanded steel meshes. Six short concrete columns, including four strengthened specimens, were tested. It was found that, unlike the bare specimens, the strengthened specimens reached their nominal flexural strengths and had good ductility factor.

Kondraivendhan and Pradhan (2009) used 15 mm thick, with a single chicken mesh layer, ferrocement laminate as external confinement to precast plain concrete cylinders of 150 mm diameter and 900 mm length (overall dimensions; diameter 180 mm; length 900 mm). Normal concrete strengths ranging from 25 to 55 MPa were tested. Results from bare specimen (150×900 mm) were compared with the confined ones and it was found that the ferrocement confinement increased the ultimate concrete compressive strengths by values up to 78%.

2. Research significance

Results from testing fifteen pipes and six roof panels made of ferrocement are presented. In addition, results found by others for three roof panels are used for comparison. Effects of the number of wire mesh layers and the dimensions of the specimens on the behaviour and ultimate moment are studied. Methods of construction and testing are discussed.

3. Loads on embedded pipes

Embedded pipes are subjected to different combination of loads; live loads due to the vehicles load and dead loads due to the soil above the pipes and hoop pressure, etc. The environment where the pipe is laid has also a contribution to the dead loads; this can be seen if the pipe is laid in an offshore where wave's loads are significant on uneven seabed. In addition to the above transverse (vertical) loads, the pipe may be subjected to axial loads. The forces causing such loads are highly variable, localized, and may not lend themselves to quantitative analysis with any degree of confidence. Some of the major causes of axial loads or beam action in a pipeline are: non-uniform bedding support, differential settlement, and ground movement such as earthquakes or frost heave. Pipe should be designed so that it can sustain the most critical load situation that might occur during the pipe lifetime. Usually, subsurface pipes are embedded between one to three meters deep. Pipes laid under agricultural land will probably be subjected only to the comparatively light vehicles operating over such ground, whereas under main highway or where road construction, the weights of the heaviest vehicles are likely to be much higher. In this research, ferrocement pipes are assumed to be used for irrigation systems within agricultural land in order to reduce water losses due to evaporation and leakage. The pipe is assumed to be resting on its joints (say due to non-uniform bed compaction) with no proper soil support between the joints as shown in Fig. 1.

4. Material and method of construction of ferrocement pipes

Ordinary Portland cement as specified in the British Standard (1996), well-graded fine aggregate complying with the ASM-C33 (1987), and fresh potable water were used in the mortar mix. The cement-to-sand proportion was 1:2 by weight and the water/cement ratio was 0.55 by weight. The reinforcement used in this project consisted basically of two types; wire mesh layers and four steel bars. The mesh was made of galvanised iron with wire diameter of 0.62 mm and opening spacing of 12.16 mm in both directions. The steel bar was 6 mm diameter mild steel with tensile yield stress of 250 MPa. The steel bars were used in order to hold the mesh in position and to give added stiffness and impact resistance; they were placed at the four quarter points of the pipe cross-section's

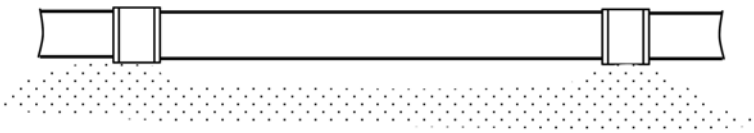

Fig. 1 Embedded pipe supported at the joints

perimeter. The cylindrical shape of the pipe was obtained by using a mould made of: (a) wooden inner core with simple collapsible system, and (b) an outer skin made of Glass Reinforced Plastic, GRP. The outer skin is made of three equal segments of about 667 mm long each in order to ease the construction process and give the 2 m length required. The wall thickness of the pipe was 20 mm including about 4 mm cover at each side of the wire mesh. The construction process constituted; first: the inner wooden core was covered with Polythene sheet for ease of dismantling, second: the steel bars were tied to the wire mesh at required locations, third: the inner core was encased with the wire mesh and the rods, fourth: the first segment of the outer skin was assembled around the inner core and the wire mesh, fifth: the mortar was poured until the top of the first

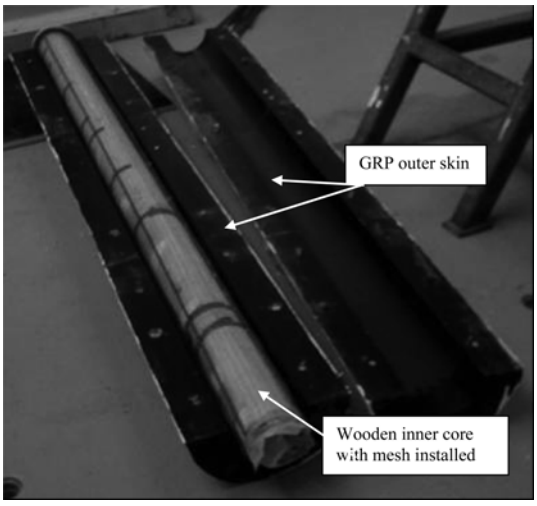

Fig. 2 Inner wooden mould with wire mesh installed and outer GRP mould

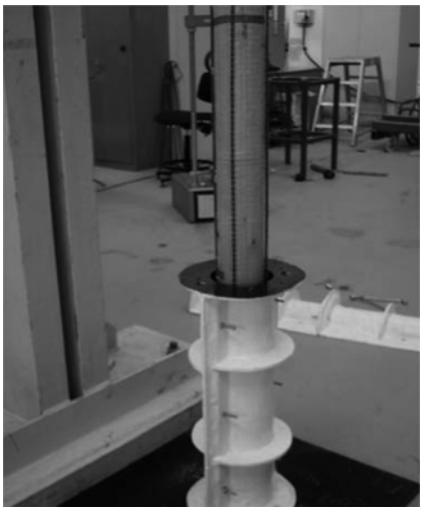

Fig. 3 Inner and outer moulds with wire mesh and steel bars installed

Fig. 4 Pipe after dismantling of moulds

segment, sixth: the second segment of the outer skin was installed and the process was repeated. Figs. 2, 3 show the inner core and the outer skins, and the wire mesh respectively. When the mortar was poured in the 20 mm gap between the inner core and the outer skin a special electrical external vibrator was used to push the mortar around the reinforcement. As this was done, great care was taken to avoid leaving air pockets and ensure that the wire mesh layers and the steel bars have internal concrete cover of about 4 mm. Three cubes (100×100×100 mm), three cylinders (150×300 mm) and two prisms (100×100×500 mm) were cast from the same mix for each specimen. One day after casting, the GRP skin and the wooden core were dismantled and the specimen and samples were cured using wet Hessian cloths for five days and then left under room condition until the date of testing. Fig. 4 shows a cast specimen with the inner wooden core and outer skin being dismantled.

5. Pipe instrumentation and testing procedure

All pipes were tested for flexure as simply supported beams using the British Standard 5911 Part 100 (1989) and Hauch and Young (1999) with a clear span of 1800 mm by applying two points load in the transverse direction of pipe longitudinal axis to produce pure bending at the middle

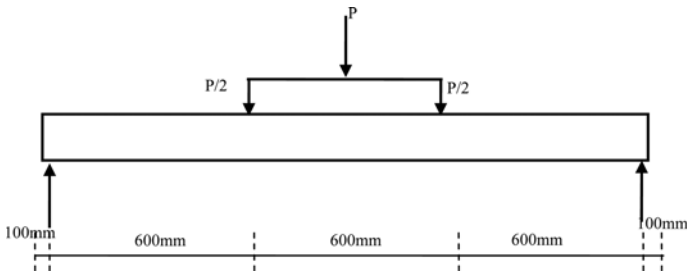

Fig. 5 Pure bending test

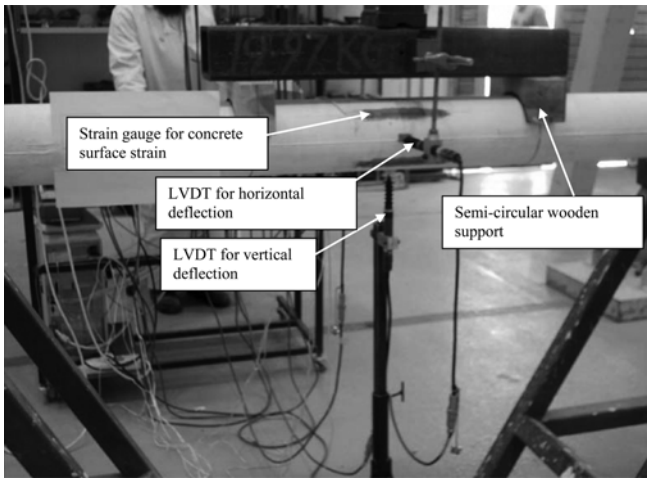

Fig. 6 Typical pipe with instrumentation

Table 1 Pipes material properties

Pipe	Pipe inner diameter	No. of mesh layers	Pipe weight	f_{cu}	f_c'	f_t'
No.	mm	Nos	kg	MPa	MPa	MPa
105-1	105	1	37.8	40.3	36.3	3.7
105-2	105	2	38	45.1	38.5	3.8
105-3	105	3	38.2	52.02	49.3	5.62
105-4	105	4	38.4	45.3	38.7	4.0
105-6	105	6	38.1	44.2	37.9	3.6
Average for 105 mm Dia.			38.1	45.38	40.14	4.14
210-1	210	1	69.2	46.2	38.63	5.52
210-2	210	2	69.0	42.1	37.4	4.23
210-3	210	3	69.1	47.8	39.1	4.6
210-4	210	4	69.1	48.0	40.2	4.45
210-6	210	6	69.0	48.3	41.05	4.5
Average for 210 mm Dia.			69.08	46.48	39.28	4.66
315-1	315	1	100.0	47.53	38.9	4.50
315-2	315	2	100.0	45.0	40.6	4.7
315-3	315	3	100.0	46.8	38.4	3.9
315-4	315	4	100.2	47.4	38.6	4.0
315-6	315	6	100.1	49.05	41.7	4.1
Average for 315 mm Dia.			100.06	47.156	39.64	4.24
Average for all specimens				46.34	39.69	4.35

600 mm test span (Fig. 5). Load was applied as two symmetrically arranged concentrated loads using a steel beam spreader and 5-ton hydraulic actuator connected to an electric load cell of 50 kN capacity. It was applied gradually in increments of 0.25 kN each. The load was transferred to the pipe through semicircular wooden load-transducers (Fig. 6). Rubber gasket where provided between the wooden load-transducers and the pipe section to ensure smooth transition of load to the pipe. Similar arrangement was used at the bottom supports. At each load increment, the pipe was checked against any developed cracks. Three Linear Variable Differential Transducers, LVDT, were used to monitor vertical and horizontal deformations. The vertical deflection was measured at the bottom of the pipe at mid-span using one LVDT while the horizontal deflection was the average values of two LVDTs installed at the front and rear faces at mid-span. For data acquisition, the LVDTs and the load cell connected to a data logger which was connected to a computer. Crack development was monitored using a glass magnifier and a crack width measuring microscope. Cracks were marked at each load increment and given the load value.

At the same day of testing the beam, the cubes were tested for compressive strength, the cylinders were tested for compressive and tensile strengths and the prisms were tested for tensile strength. Table 1 shows the properties of specimen and measured average material properties of tested pipes.

Table 2 Effect of number of wire mesh layers on cracking and ultimate moments

1	2	3	4	5
Pipe	Cracking Moment	Percentage of increase in cracking moment	Ultimate Moment	Percentage of increase in Ultimate Moment
No.	kNm	%	kNm	%
105-1	2.3	-	2.55	-
105-2	3.2	39.1	3.4	33.3
105-3	3.5	52.2	4.3	68.6
105-4	4	73.9	5.1	100
105-6	4.2	82.6	4.6	80
210-1	6.1	-	8.41	-
210-2	7.8	27.9	8.4	0
210-3	8	31.1	8.42	0
210-4	8.2	34.4	9.33	10.9
210-6	11.6	90	12.8	52.2
315-1	8.3	-	9.10	-
315-2	9.3	12	9.64	5.93
315-3	11.8	42	12.67	39.2
315-4	14.1	70	17.18	88.8
315-6	13.9	67.5	16.66	83.0

6. Pipes' test results

A ferrocement pipe reinforced with wire mesh layers and subjected to an increase of pure bending moment will fail as a result of flexural cracks or loss of resistance due to change of cross sectional shape from circular to oval (bulging), based on the amount of reinforcement.

In this section, the effects of the number of mesh layers and the diameter of the pipe on the vertical deflection and section distortion, concrete surface strains and failure loads are presented. Table 2 shows the measured cracking moment, failure moment, vertical deflection and pipe distortion at mid-span of each pipe.

6.1 Effects of number of wire mesh layers

6.1.1 Cracking and ultimate moments

Column 2 of Table 2 shows that the increase in the number of wire mesh layers led to increase in the cracking moment in all pipes. This is due to the increase in tensile strength of concrete caused by the increased number of wire mesh layers. This is different than the case of conventional reinforced concrete, where the concrete dimensions are relatively much larger than the dimensions of the reinforcing bars, concrete determines the cracking moment of the section, and hence, the cracking load is almost not influenced by the quantity of steel provided. Column 3 of Table 2 shows the percentage of increase in cracking moment with respect to the pipe with one mesh layer among the members of each series. The values show almost linear increment in each series for the given

values. In all tested pipes, it was found that almost vertical cracks start at the bottom face of the pipe near mid-span and then extend into the upper sides with the succeeding load increments. The spacing between cracks was reduced with the increase in the number of wire mesh layers. The cracks also became thinner and lesser in number with the increase in the number of wire mesh layers. Fig. 7 shows cracks of typical tested specimens.

Fig. 8 shows that, in general, the ultimate moment increases as the number of wire mesh layers increases. Column 5 of Table 2 shows the percentage of increase in the ultimate moment with respect to the pipe with one mesh layer among the members of each series. Similar to the cracking moment; almost linear increment values in each series can be visualized. It is clear that the differences between the cracking moments and the ultimate moments for each pipe diameter was not large which indicates that after cracking, the wire mesh layers have less effect on strength.

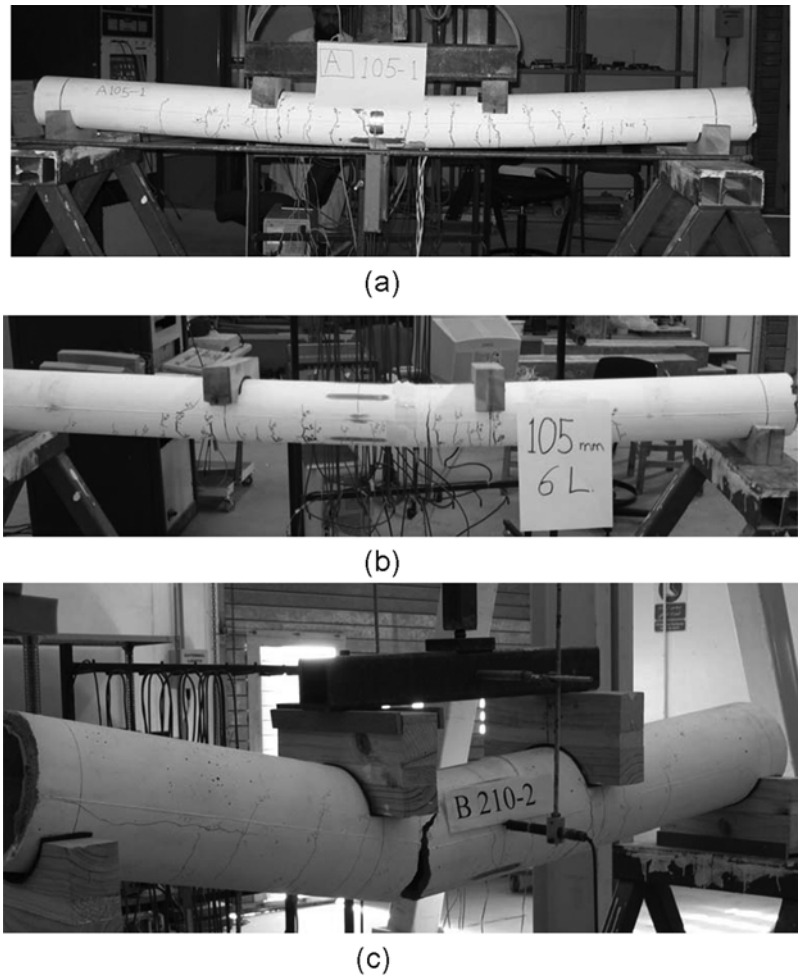

(a)

(b)

(c)

Fig. 7 (a) Tested pipe 105-1, (b) Tested pipe 105-6, (c) Tested pipe 210-2, (d) Tested pipe 210-6, (e) Tested pipe 315-4

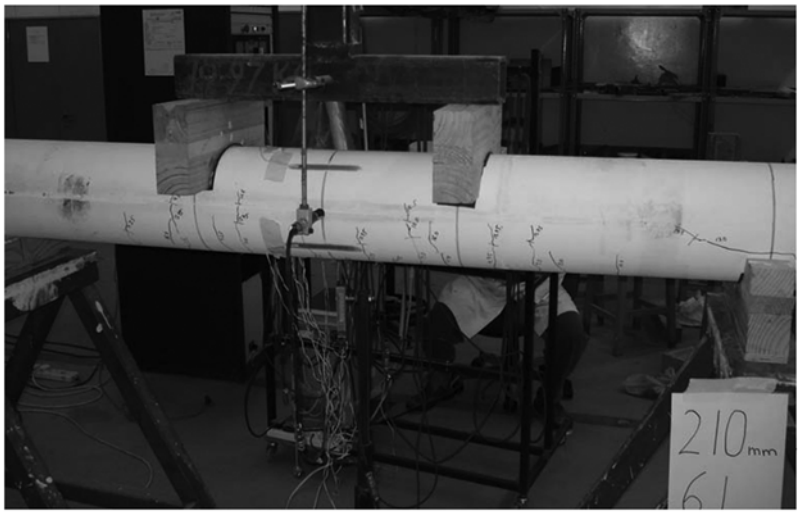

(d)

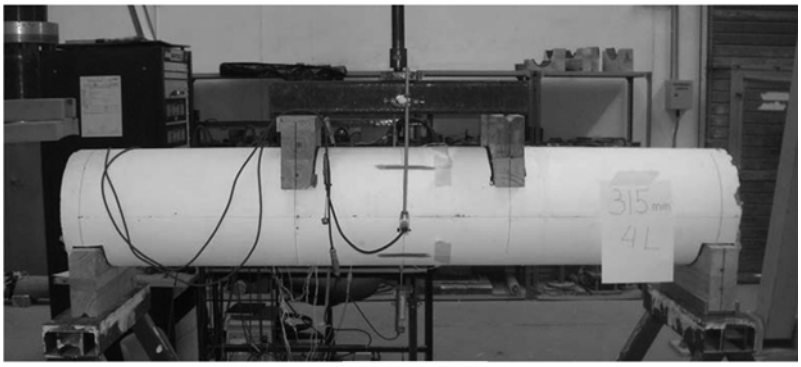

(e)

Fig. 7 Continued

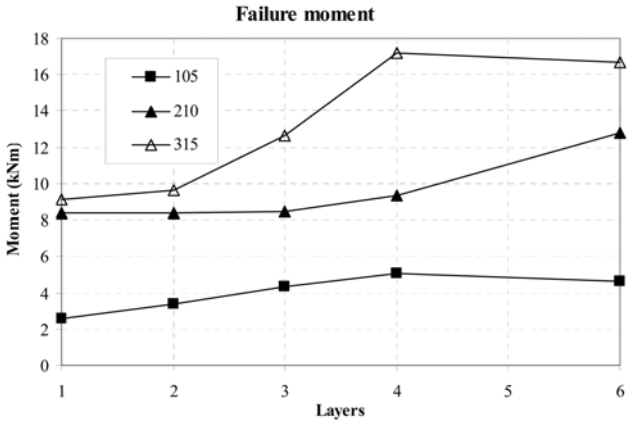

Fig. 8 Effect of number of wire mesh layers on the pipe failure moment

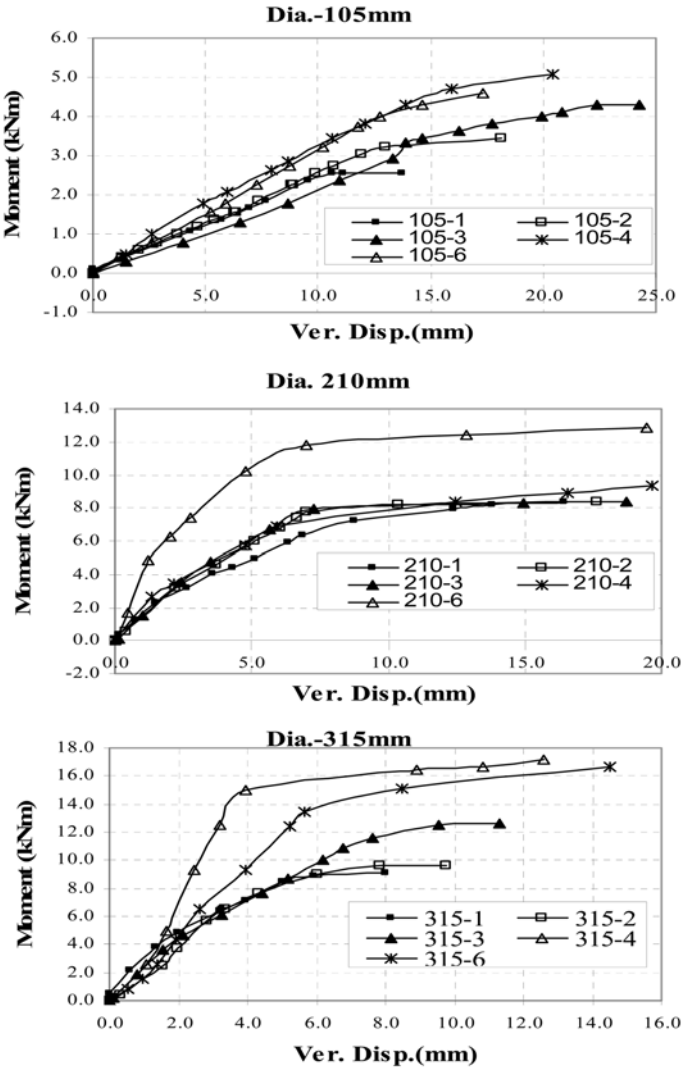

Fig. 9 Effect of the number of wire mesh layers on the pipe vertical deflection

6.1.2 Vertical deflection at mid-span

From Fig. 9 it can be stated that, in general, increasing the number of wire mesh layers increases the pipe stiffness (less displacement for the same load) and increases the ultimate moment. The effect was more pronounced in the case of 315-series. Column 2 of Table 3 shows the vertical deflection measured at the bottom face of the section at mid-span.

6.1.3 Section distortion

No major distortion (horizontal deflection) was recorded by the LVDTs installed on the pipe sides as can be seen from column 3 of Table 3.

Table 3 Pipes vertical and horizontal displacements

1	2	3
Pipe No.	Max. Vertical Deflection, mm	Max. Horizontal Deflection, mm
	mm	mm
105-1	13.75	0.17
105-2	18.13	0.2
105-3	24.25	0.38
105-4	20.45	0.06
105-6	17.31	0.13
Average for 105	18.78	0.19
210-1	16.4	0.04
210-2	17.65	0.11
210-3	18.75	0.08
210-4	19.64	0.04
210-6	19.45	0.20
Average for 210	18.38	0.09
315-1	7.98	0.32
315-2	9.79	0.25
315-3	11.30	0.09
315-4	12.59	0.15
315-6	14.52	0.147
Average for 315	11.24	0.19

6.2 Effects of pipe diameter

6.2.1 Cracking and ultimate moments

From Fig. 10 it is clear that increasing the diameter increases the cracking moment. This is due the fact that the cracking moment is proportional to the outer diameter of the pipe (effect of the moment of inertia) as shown below:

$$M_{cr} = \frac{\sigma_{\max} I}{y_{\max}}$$

$$= \left\{ \frac{\pi}{64}(d_o^4 - d_i^4) f_t' \right\} / (d_o/2) \text{ where: } y_{\max} = d_o/2 \text{ and } \sigma_{\max} = f_t'$$

$$= \frac{\pi}{32} f_t' \left(d_o^3 - \frac{d_i^4}{d_o} \right) \text{ put } d_i = n d_o$$

$$= \frac{\pi}{32} f_t' d_o^3 (1 - n^4)$$

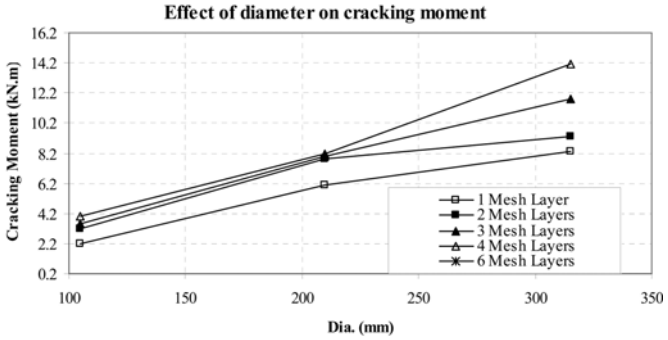

Fig. 10 Effect of the pipe diameter on the cracking moment

Example: for plain concrete with $f_t' = 3$ MPa and varying diameter, the following result can be found:

d_i (mm)	d_o (mm)	$d_i/d_o = n$	$1 - n^4$	M_{cr} (kNm)
200	240	0.833	0.518	2.108
300	340	0.882	0.394	4.559
400	440	0.909	0.317	7.953
500	540	0.926	0.265	12.289

The percentage increase in the cracking moment with respect to those of the smallest diameter

Table 4 Effect of pipe diameter on cracking and ultimate moments

1	2	3	4	5
Pipe	Cracking Moment	Percentage of increase in cracking moment	Ultimate Moment	Percentage of increase in Ultimate Moment
No.	kNm	%	kNm	%
105-1	2.3	-	2.55	-
210-1	6.1	165.2	8.41	229.8
315-1	8.3	260.9	9.10	256.9
105-2	3.2	-	3.4	-
210-2	7.8	143.8	8.4	147
315-2	9.3	265.2	9.64	183.5
105-3	3.5	-	4.3	-
210-3	8	128.6	8.42	95.8
315-3	11.8	237.1	12.67	194.65
105-4	4	-	5.1	-
210-4	8.2	105	9.33	82.9
315-4	14.1	252.5	17.18	236.9
105-6	4.2	-	4.6	-
210-6	11.6	176.2	12.8	178.3
315-6	13.9	231	16.66	262.2

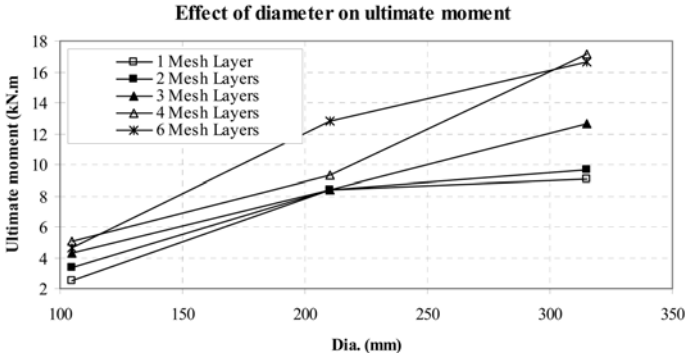

Fig. 11 Effect of the pipe diameter on the ultimate moment

(105 mm) are shown in column 3 of Table 4. In general, the increase in the cracking moment when the diameter was increased from 105 mm to 210 mm was more than the increase when the diameter was increased from 210 mm to 315 mm. In all cases, the increase in the cracking moment due to the increase in the pipe diameter was very significant.

Column 4 of Table 4 shows that the ultimate moment increases as the pipe diameter increases for the same number of wire mesh layers. This is due to the effect of larger lever arm. The percentage increase in the ultimate moment shown in column 5 with respect to the 105 diameter pipe shows that ultimate moment vary considerably and no general trend could be visualized among the members of each number of wire mesh layers. Fig. 11 also shows that the larger the diameter the larger the failure moment, with all numbers of layers of mesh. This is obvious, as little difference between the cracking moment and the ultimate moment.

6.2.2 Vertical deflection at mid-span

From Fig. 12 it is clear that the larger the diameter, the stiffer (less displacement for same load) the behaviour. In general, reduction in displacement was more pronounced when the diameter was increased from 105 mm to 210 mm than when it was increased 210 mm to 315 mm.

7. Material and method of construction of ferrocement roof panels

The experimental investigation consisted of fabricating and testing, for flexure, nine ferrocement roof panels. All panels were 20 mm thick and were reinforced with thin steel wire meshes sandwiched midway through the thickness. The panels were divided into three groups according to their shape, number of wire mesh layers and depth of edge beams (Table 5). The first group, Channel ChA, consisted of three channel-shaped panels. The dimensions were 470 mm outer widths and 2100 mm length with two edge beams 95 mm deep (Fig. 13). The second group, Channel ChB, (Hago *et al.* 2005) consisted of three channel-shaped panels similar to the first group except that the edge beam was 50 mm deep (Fig. 14). The third group consisted of three box section panels with 470×95 mm outer cross section and 2100 mm total length. The hollow core was 430×55 mm (Fig. 15). In all tested panels, the test span was the middle 600 mm of the span.

Ordinary Portland cement and natural sand were used in making the ferrocement concrete in the ratio of 1:2; respectively with a water to cement ratio of 0.55. Along with each panel, three

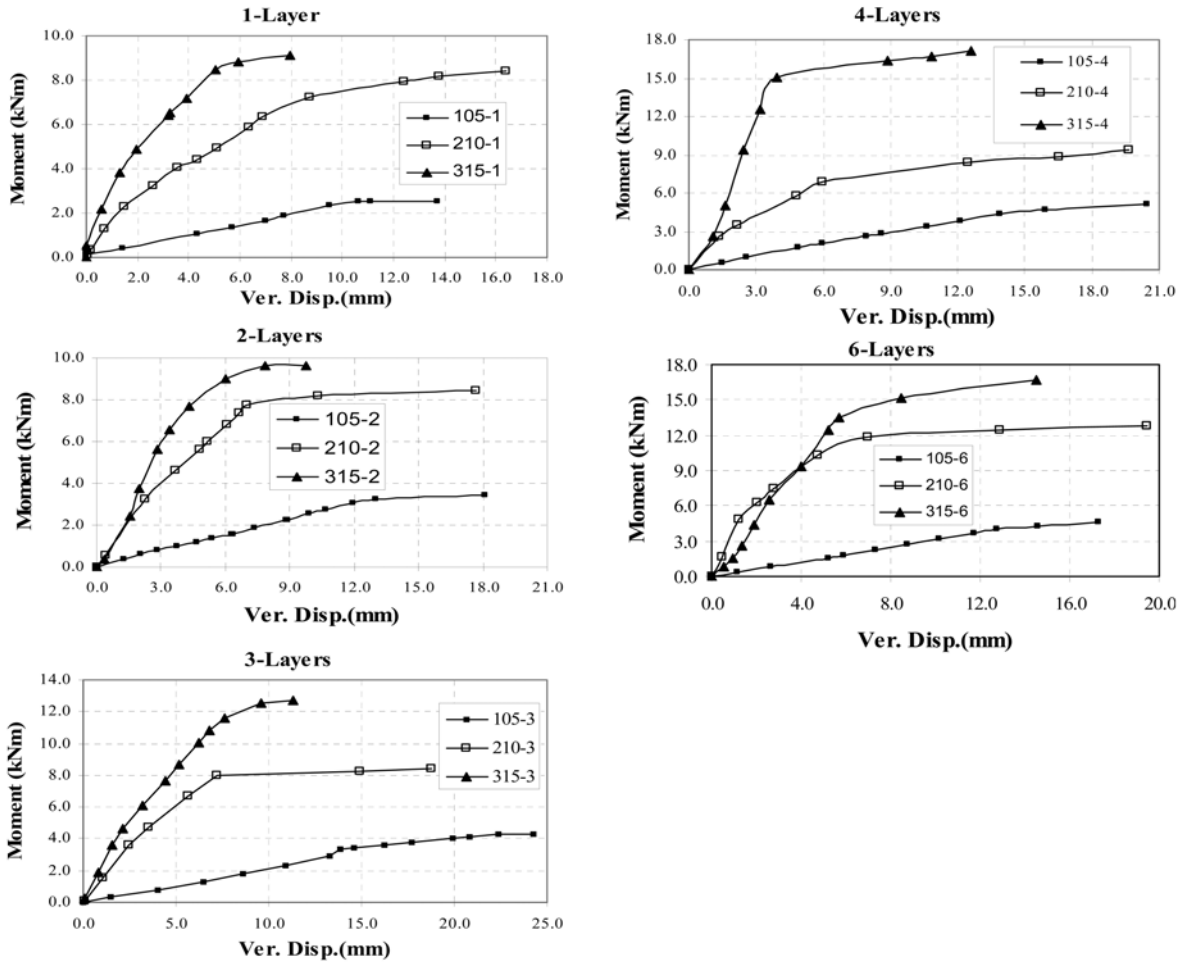

Fig. 12 Effect of the diameter size on pipe vertical deflection

Table 5 Panel models tested and their material properties

Model No.	Dimensions (mm)	Depth of edge beam (mm)	No. of steel layers	% Volume of steel	Compressive strength f_{cu}, (MPa)	Flexural strength f_r (MPa)
ChA-2	2100×470×20	95	2	1.36	54.9	5.0
ChA-4	2100×470×20	95	4	1.60	46.0	4.8
ChA-6	2100×470×20	95	6	1.76	47.5	4.6
ChB-2*	2100×470×20	50	2	1.36	42.6	6.6
ChB-4*	2100×470×20	50	4	1.57	40.6	6.8
ChB-6*	2100×470×20	50	6	1.77	42.0	6.6
Box-2	2100×470×20	95	2	1.24	44.1	5.8
Box-4	2100×470×20	95	4	1.43	31.0	5.5
Box-6	2100×470×20	95	6	1.62	54.6	7.2

*Hago *et al.* (2005).

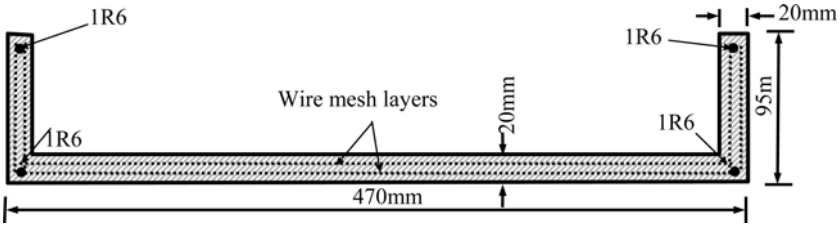

Fig. 13 Cross-sectional geometry of channel section ChA

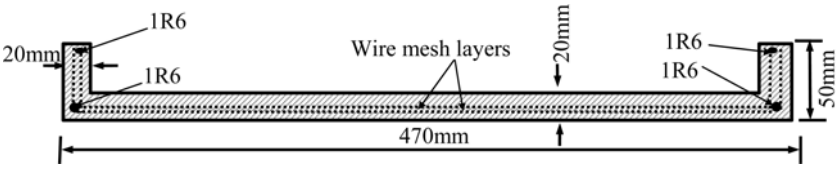

Fig. 14 Cross-sectional geometry of channel section ChB

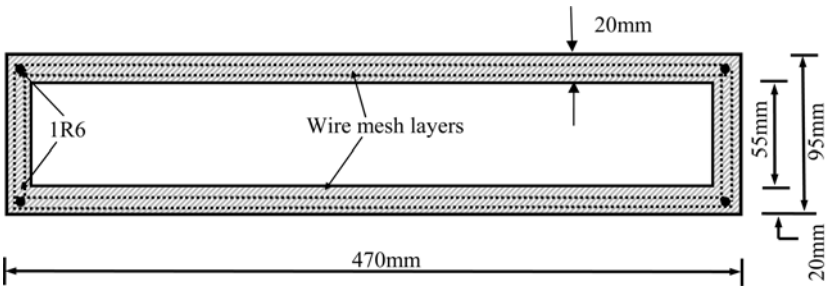

Fig. 15 Cross-sectional geometry of Box section

Fig. 16 Method of construction of a typical panel

100×100×100 mm cubes and two 100×100×500 mm prisms were cast to determine the mortar compressive strength and modulus of rupture. After one day of casting, the panels and cubes were removed from the moulds and were cured under wet Hessian cloth for three days and then kept under room condition until the date of testing which was about 28 days from the date of casting. The average mortar cube compressive strength was 47.1 MPa and the average tensile flexural strength was 5.23 MPa (Table 5). For reinforcement, a galvanised iron wire mesh with closely spaced wires was used in the tested panels. The wire mesh had a diameter of 0.62 mm and a

spacing of 12.16 mm in both directions. The number of wire mesh layers varied from two layers to six layers. The wire mesh was stretched on a frame of 6 mm steel bars having yield stress of 250 MPa. The cement, sand and water were mixed using a power driven drum mixer for about five minutes. Wooden moulds were used to cast the slabs. A layer of mortar of about 10 mm thick was first placed in the mould followed by the reinforcement cage and then a second layer of mortar was placed to make the required thickness. Due to the small thickness of the panel, the wire mesh was placed almost at mid thickness. Fig. 16 shows typical panel under construction.

8. Testing procedure

All slabs were tested for flexure. They were simply supported with a clear span of 2000 mm and test span of 600 mm in mid-span as shown in Fig. 17. The load was applied as two symmetrically arranged concentrated loads, using a spreader steel beam and a 50 kN hydraulic jack. The load was measured using an electric load cell of 50 kN capacity and was applied in increments of 0.25 kN. The slabs were painted using white emulsion to assist in detecting the cracks. Deflection under the centre of the slab was measured using Linear Variable Deferential Transducers (LVDT). The load cell and LVDT were connected to a data acquisition system. At each load increment, careful search was made for cracks on all sides of the slab with the aid of a magnifying glass and a powerful

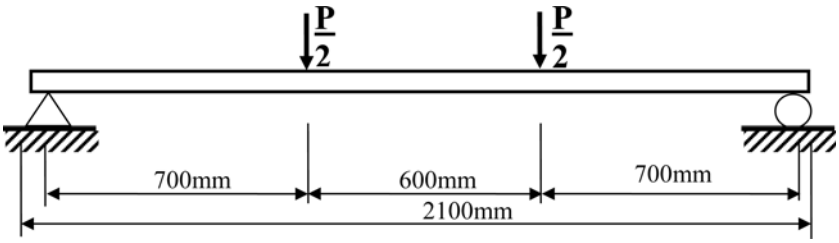

Fig. 17 Loading and support arrangements

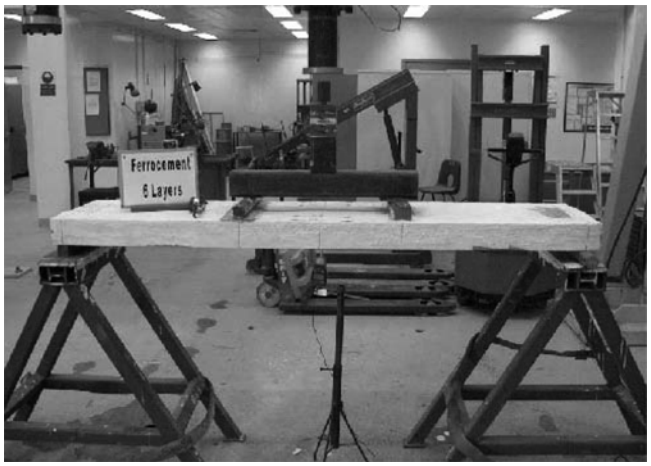

Fig. 18 Test rig and typical panel tested

electric lamp. The crack spacing, the number of cracks, the extent of the cracked zone over the length of the slab and the ultimate load were all noted. The failure load recorded in this investigation was the load value after which the panel ceases to resist additional load or the load measured just before sudden collapse. The three cubes and the two prisms were tested at the same day of testing their corresponding panel for compressive and flexural strengths respectively. Fig. 18 shows typical tested panel.

9. Panels' test results

Table 6 shows the measured values of cracking and ultimate moments, the measured vertical deflection at mid-span and observed numbers and intensities of surface cracks of the tested panels. The results are discussed in the following sub sections.

9.1 Cracking and ultimate moments

Fig. 19 shows that the general trend shows an increase in the cracking moment with the increase in number of wire mesh layers in all shapes. This is possibly due to the same reasoning given in section 6.1.1. It can also be seen from this Fig. that the section shape has no significant effect on the cracking moment. Fig. 20 shows typical crack pattern in a box section.

Fig. 21 shows that the ultimate moment increased with the increase of the number of wire mesh layers in all shapes. The increment was less pronounced in the case of channel ChB. The box section and channel ChA section had almost similar values of failure moments which were higher than the failure moments of the channel ChB sections for all number of layers. This indicates that the edge beam has major effect on the ultimate moment of resistance.

Table 6 Results of the service and ultimate behaviour of the ferrocement panels

Model No.	Cracking Moment (kNm)	Ultimate Moment (kNm)	Max. Central deflection (mm)	Surface cracks		
				No. of cracks	Distance covered by cracks (mm)	Average spacing between cracks (mm)
ChA-2	0.581	1.925	43.86	37	1150	31.08
ChA-4	0.875	1.981	36.65	71	1240	17.5
ChA-6	1.281	3.031	22.33	120	1440	12
ChB-2*	0.56	1.057	34.62	7	980	140
ChB-4*	0.998	1.6695	50.42	10	1000	100
ChB-6*	0.999	1.785	56.60	9	840	93.3
Box-2	0.651	1.89175	41	29	1100	37.93
Box-4	0.864	2.2638	25.19	38	1250	32.89
Box-6	1.379	3.304	18.64	80	900	11.25

*Hago *et al.* (2005)

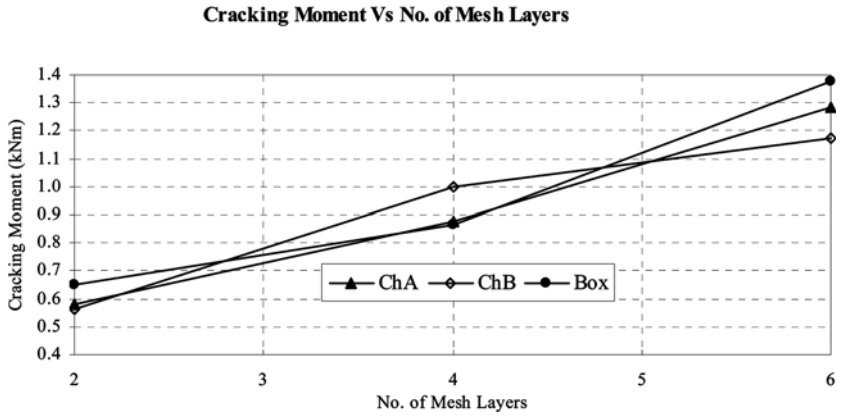

Fig. 19 Effect of the number of mesh layers on the panel cracking moment

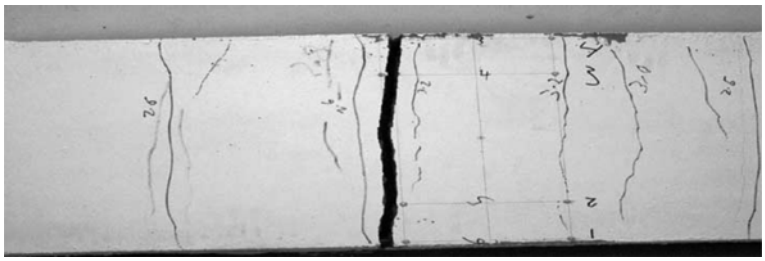

Fig. 20 Typical crack pattern in a box section

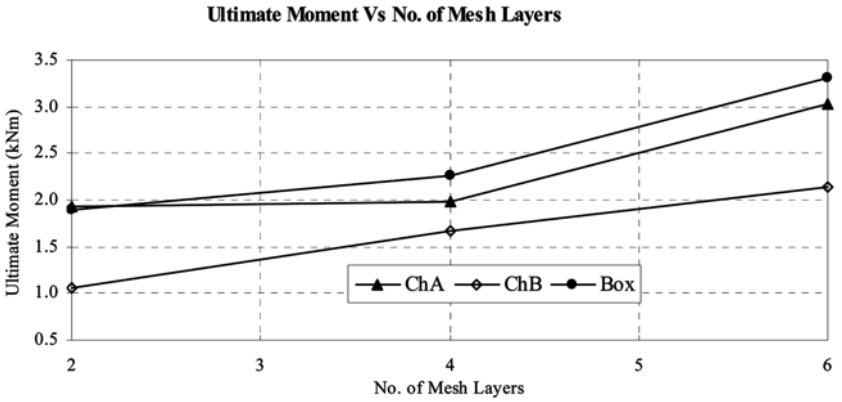

Fig. 21 Effect of the number of mesh layers on the panel ultimate moment

9.2 Vertical deflection at mid-span

Fig. 22 shows the effect of the number of wire mesh layers on the moment-deflection curves. It is clear that in all panels, as the number of wire mesh layers increases the stiffness increases (less deflection for the same load). Fig. 23 shows the effect of the cross-sectional shape on the load-

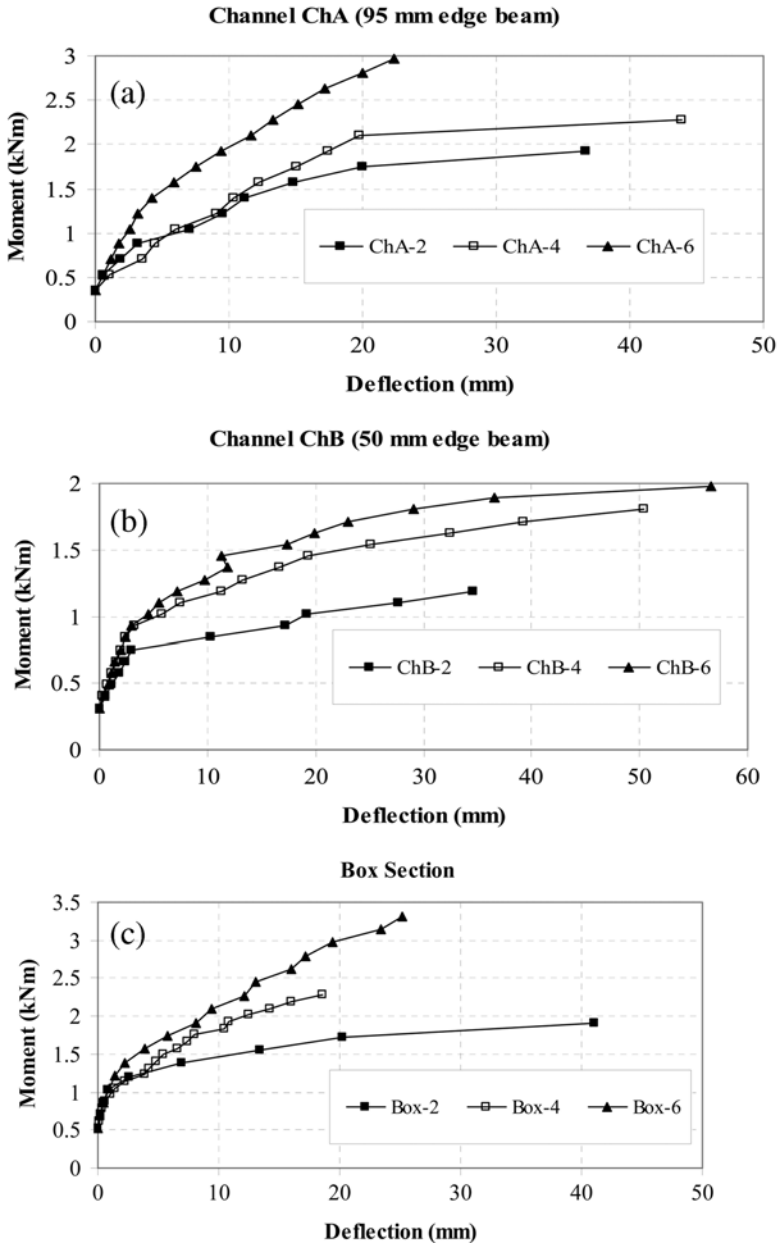

Fig. 22 Effect of the number of wire mesh layers on deflection (a) Moment-deflection (ChA), (b) Moment-deflection (ChB), (c) Moment-deflection (Box section)

deflection curves. It is clear that there are no major differences in the behaviour of channel ChA and box section while channel ChB behaved in a softer manner, having more deflection than the box section or channel ChA for same load. This indicates that the edge beam plays major effect on the deflection of the panel.

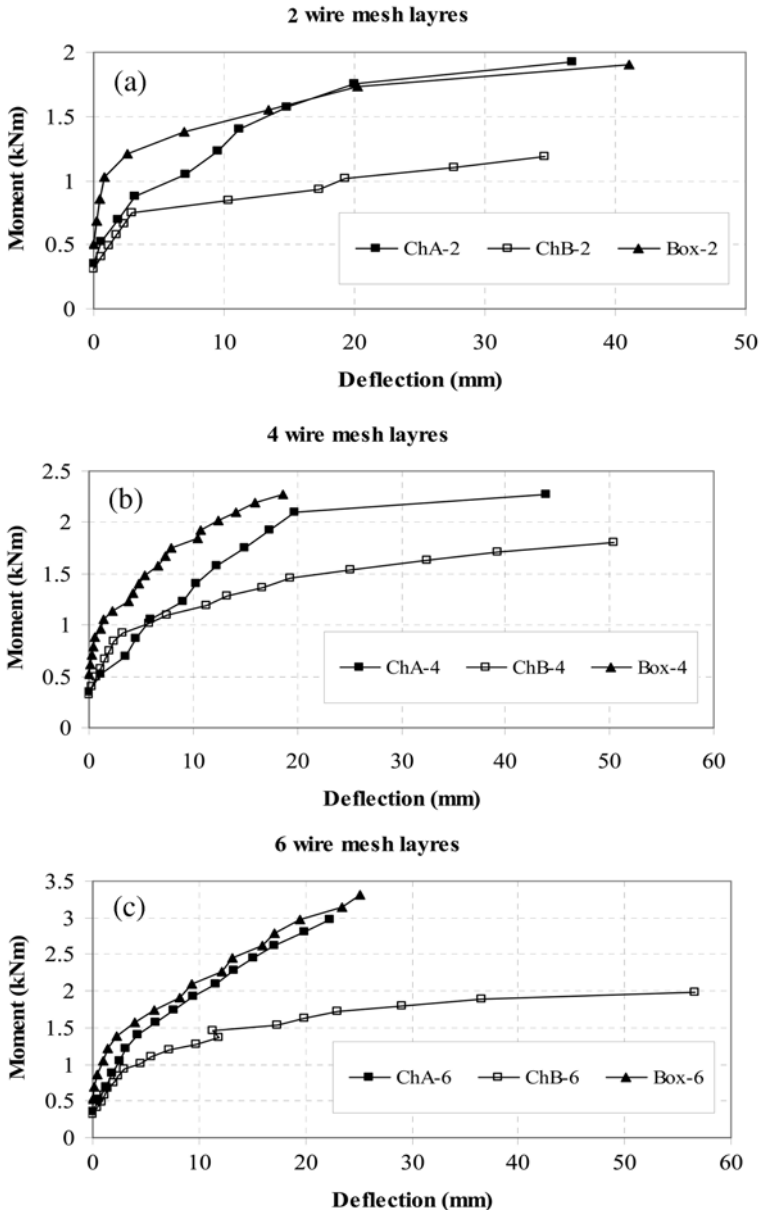

Fig. 23 Effect of cross sectional shape on deflection of panels. (a) Moment-deflection (2 wire mesh layers), (b) Moment-deflection (4 wire mesh layers), (c) Moment-deflection (6 wire mesh layers)

10. Remarks on the test results

The test results presented in sections 6 and 9 can be summarised as follows:

1. Increasing the number of wire mesh layers increases the cracking and ultimate moments.
2. Increasing the diameter of the pipe increases the cracking and ultimate moments. The effect of the diameter was more pronounced than the effect of the wire mesh layers.

3. In all tested pipes, the horizontal distortions were negligible.
4. Increasing the depth of the edge beam increases ultimate moment of resistance.
5. The box section and the channel section with the same depth i.e. ChA and Box behaved in a very similar fashion when the number of wire mesh is the same.
6. In most specimens tested, three stages of behaviour until failure:
   a) Pre-cracking stage: both concrete and steel materials were elastic and moment-deflection curve was almost linear in most cases. The larger the number of mesh layers, the lesser was the deflection for the same load. This was possibly due to the fact that larger area of reinforcement helped on producing stronger bond. Few fine cracks were developed during this stage but did not cause major changes in the behaviour. As was expected, increasing the diameter of the pipe or the depth of the edge beam increased the moment of inertia and the lever arm which led to larger cracking and ultimate moments. This stage was ended by the cracks induced at the bottom of the specimen near mid-span.
   b) Multiple cracking stage: during this stage large number of vertical and inclined cracks developed and the load was transferred from concrete to the wire meshes. The wire mesh elongated under additional load, thus transferring the load back to the concrete matrix, thereby producing new cracks. The load resistance of the specimen was increased by the increase in the number of wire mesh layers or by the increase of the pipe's diameter or the depth of panel's edge beam.
   c) Failure stage: this stage was indicated by intensification of existing cracks with the increase in load. The tensile stress was mainly carried by the mesh and the longitudinal steel bars. The pipe exhibited large vertical deflection at failure. All specimens showed ductile mode of failure.

11. Conclusions

Fifteen pipes and nine roof panels made of ferrocment were tested for pure bending. The wall thickness for all pipes and panels was 20mm. Ordinary Portland cement, natural sand, orthogonal direction wire mesh and mild steel bars were used for construction. The main variables studied were the number of wire mesh layers (1, 2, 3, 4 and 6), the pipe diameter (105, 210, 315 mm), the cross-sectional shape of the roof panel (Channel or Box) and the depth of the edge beam for the panels (95 or 50 mm). It was observed that as the percentage of the reinforcement increases; the ultimate bending moment increases. It was also observed that increasing the percentage of the reinforcement results in reduction in the number and width of cracks. Most of the pipes and panels underwent ductile behaviour until failure.

The increase in pipe diameter led to increase in the cracking moment, ultimate moment and the stiffness. Increasing the pipe diameter produces greater effect than increasing the number of wire mesh layers.

Results from two types of channel section, channel ChA and channel ChB, differing in the depth of the edge beam (95 mm and 50 mm respectively) and one type of Box section (95 mm overall depth) were compared. It was observed that the use of a ferrocement box section in the panels does not provide significant improvement in the strength than the use of channel sections of the same depth and wire mesh layers. Noting that box sections are more difficult to manufacture than channel sections, it is advisable, given the choice, to use a channel section unless other factors are considered i.e. heat insulation.

References

Abdullah and Takiguchi K. (2003), "An investigation into the behaviour and strength of reinforced concrete columns strengthened with ferrocement jackets", *Cement Concrete Compos*., **25**(2), 233-242.

ACI Committee 549 (1997), State-of-Art Report on ferrocement, American Concrete Institute, ACI-R97, Manual of Concrete Practice, p. 26, Farmington Hills, MI, 48333-9094, USA.

ACI Committee 549 (1993), Guide for Design, Construction and Repair of Ferrocement ACI 549 IR-93, Manual of Concrete Practice, p. 27, American Concrete Institute, Farmington Hills, MI, 48333-9094, USA.

Al-Sulaimani, G.J. and Ahmad, S.F. (1988), "Deflection and flexural rigidity of Ferrocement I and Box beam", *J. Ferrocement*, **18**(1), 1-12.

ASTM-C33 (1987), "Specification for concrete aggregate", USA.

British Standard 12 (1996), Specification for Portland Cement, British Standard Institution, 389Chiswick High Road, London, W4 4AL BSI London, UK.

British Standard 5911: Part 100 1989, Specification for Precast Concrete Pipes, Ancillary and Products, British Standard Institution, 389Chiswick High Road, London, W4 4AL.

Duggal, S.K. (1998), "Bamboo ferrocement water supply pipes", *Indian Concrete J.*, **72**(8), 413-416.

Greepala, V. and Nimityongskul, P. (2008), "Structural integrity of ferrocement panels exposed to fire", *Cement Concrete Compos*., **30**(5), 419-430.

Hago, A.W., Al-Jabri, K.S., Al-Nuaimi, A.S., Al-Moqbali, H. and Al-Kubaisy, M.A. (2005), "Ultimate and service behaviour of ferrocement roof slab panels", *Construct. Build. Mater.*, **19**(1), 31-37.

Hauch Soren and Yong Bai (1999), "Bending moment capacity of pipes", Offshore Mechanical and Arctic Engineering, July 11-16, 3.

Iorns, M.E. (1989), "OTEC seawater pipe cost comparisons", *Proc. of the First International Conference on Ocean Energy Recovery ICOER'89*, Honolulu, Hawaii, 28-30 November, 297-306.

Ismail, M.S. and Waliuddin, A.M. (1996), "Network ferrocement drainage system", *J. Ferrocement*, **26**(2), 113-119.

Kazemi, M.T. and Morshed, R. (2005), "Seismic shear strengthening of R/C columns with ferrocement jacket", *Cement Concrete Compos*., **27**(7-8), 834-842.

Kenai, S. and Brooks, J.J. (1994), "Tensile, flexural and impact behaviour of ferrocement with chicken wire mesh reinforcement", *Proceedings of the Fifth International Symposium on Ferrocement*, UMIST, Manchester, 342-355.

Kondraivendhan, B. and Pradhan, B. (2009), "Effect of ferrocement confinement on behaviour of concrete", *Construct. Build. Mater.*, **23**(3), 1218-1222.

Al-Kubaisy, M.A. and Jumaat M.Z. (2000), "Flexural behaviour of reinforced concrete slabs with ferrocement tension zone cover", *Construct. Build. Mater.*, **14**(5), 245-252.

Mansur, M.A., Ahmed I. and Paramasivam, P. (2001), "Punching shear strength of simply supported ferrocement slabs", *J. Mater. Civil Eng.*, **13**(6), 418-426.

Mansur, M.A. and Paramasivam, P. (1985), "Cracking behaviour and ultimate strength of ferrocement in flexure", *Proceedings of the Second International Symposium on Ferrocement*, Bangkok, Thailand, 47-59.

Mathews, M.S., Sudhakumar, J., Sheela, S. and Seetharaman, P.R. (1991), "Analytical and experimental investigations of hollow ferrocement roofing units", *J. Ferrocement*, **21**(1), 1-14.

Masood, A., Arif, M., Akhtar, S. and Haquie, M. (2003), "Performance of ferrocement panels in different environments", *Cement Concrete Res.*, **33**(4), 555-562.

Memon, N.A., Sumadi, S.R. and Ramli, M. (2007), "Performance of high workability slag-cement mortar for ferrocement", *Build. Environ.*, **42**(7), 2710-2717.

Moita, G.F., Las Casas, E.B. and Carrasco, E.V.M. (2003), "Experimental and numerical analysis of large ferrocement water tanks", *Cement Concrete Compos*., **25**(1), 243-251.

Paramasivam, P., Lim, C.T.E. and Ong, K.C.G. (1998), "Strengthening of RC beams with ferrocement laminates", *Cement Concrete Compos*., **20**(1), 53-65.

Sander, J., Kacprzyk, B. and Kacprzyk, Z. (1985), "Ferrocement covers for district heating pipes", *J. Ferrocement*, **15**(4), 343-347.

Shannag, M.J. (2008), "Bending behaviour of ferrocement plates in sodium and magnesium sulphates solutions",

Cement Concrete Compos., **30**(7), 597-602.
Shui, L.T. (1989), "Ferrocement pipes for subsurface drainage", *J. Ferrocement*, **19**(1), 29-35.
Silva, A.R.C., Proenca, S.P.B., Billardon, R. and Hild, F. (2004), "Probabilistic approach to predict cracking in lightly reinforced microconcrete panels", *J. Eng. Mech*., **130**(8), 931-941.
Wei, Z. (1985), "A research on glass-fibre reinforced plastic Ferrocement (GRPF) and its application in irrigation engineering", *J. Ferrocement*, **15**(4), 359-364.
Yen, T. and Su, C.F. (1980), "Influence of skeletal steel on the flexural behaviour of ferrocement", *J. Ferrocement*, **10**(3), 177-188.